C. R. Biologies 338 (2015) 425–433

Contents lists available at ScienceDirect

Comptes Rendus Biologies

www.sciencedirect.com

Biological modelling/Biomodélisation

# Assessing the three-dimensional collagen network in soft tissues using contrast agents and high resolution micro-CT: Application to porcine iliac veins

## *Évaluation de la structure tridimensionnelle du réseau de collagène dans des tissus mous, par l'utilisation d'agents de contraste et de microtomographie haute résolution : application à des veines iliaques de porc*

Mathieu Nierenberger [a,b,*], Yves Rémond [a,b], Saïd Ahzi [a,b], Philippe Choquet [a,b,c]

[a] *ICube, équipe MMB, CNRS, université de Strasbourg, 4, rue Boussingault, 67000 Strasbourg, France*
[b] *Fédération de médecine translationnelle de Strasbourg, faculté de médecine, université de Strasbourg, 67000 Strasbourg, France*
[c] *Preclinical Imaging Lab (UF6237), pôle d'imagerie, hôpitaux universitaires de Strasbourg, hôpital de Hautepierre, 67098 Strasbourg, France*

ARTICLE INFO

*Article history:*
Received 23 June 2014
Accepted after revision 18 April 2015
Available online 29 May 2015

*Keywords:*
Collagen
Tissue stains
Vasa vasorum
Vein wall
X-Ray microtomography
Three-dimensional imaging

ABSTRACT

The assessment of the three-dimensional architecture of collagen fibers inside vessel walls constitutes one of the bases for building structural models for the description of the mechanical behavior of these tissues. Multiphoton microscopy allows for such observations, but is limited to volumes of around a thousand of microns. In the present work, we propose to observe the collagenous network of vascular tissues using micro-CT. To get a contrast, three staining solutions (phosphotungstic acid, phosphomolybdic acid and iodine potassium iodide) were tested. Two of these stains were showed to lead to similar results and to a satisfactory contrast within the tissue. A detailed observation of a small porcine iliac vein sample allowed assessing the collagen fibers orientations within the medial and adventitial layers of the vein. The vasa vasorum network, which is present inside the adventitia of the vein, was also observed. Finally, the demonstrated micro-CT staining technique for the three-dimensional observation of thin soft tissues samples, like vein walls, contributes to the assessment of their structure at different scales while keeping a global overview of the tissue.


*Mots clés :*
Collagène
Colorants
Vasa vasorum
Paroi vasculaire
Microtomodensitométrie
3D

RÉSUMÉ

La connaissance de l'architecture tridimensionnelle du réseau de collagène présent dans les parois vasculaires est primordiale pour la construction de modélisations structurelles permettant de décrire le comportement mécanique de ces tissus. La microscopie multiphotonique permet de telles observations, mais est limitée à des volumes d'observation mesurant quelques centaines de micromètres. Dans ce travail, nous proposons une observation du réseau de collagène présent dans les parois vasculaires en utilisant une technique de microtomographie X. Trois agents de contraste ont été

* Corresponding author. Laboratoire ICube, CNRS, université de Strasbourg, 4, rue Boussingault, 67000 Strasbourg, France.
*E-mail addresses:* nierenbergerm@unistra.fr (M. Nierenberger), remond@unistra.fr (Y. Rémond), ahzi@unistra.fr (S. Ahzi), pchoquet@unistra.fr (P. Choquet).

http://dx.doi.org/10.1016/j.crvi.2015.04.009
1631-0691/

comparés (acide phosphotungstique, acide phosphomolybdique et iodure de potassium). Deux de ces colorations ont mené à l'obtention d'un contraste satisfaisant dans le tissu. Des observations détaillées de petits échantillons de veines iliaques de porc ont permis d'évaluer les orientations prédominantes des fibres de collagène dans la média et l'adventice de la paroi de la veine. Le vasa vasorum présent dans l'adventice a également pu être observé. Finalement, la technique proposée utilise la microtomographie X pour évaluer l'architecture tridimensionnelle de la structure interne de fins échantillons de tissu mou, tels que des parois vasculaires. Elle permet, à une échelle supérieure, de conserver un aperçu de la structure globale du tissu.



## 1. Context and goals

The exploration of the structure of organs has remained descriptive for a long time. At the cellular scale, histology has allowed for a large amount of information about tissues structure, mainly achieved by the use of specific staining procedures. Nevertheless, the need for tissue modeling is in constant growth and requires a volume three-dimensional (3D) vision of the tissue structure at various scales. Histological techniques are not the most appropriate for this. Indeed, they associate a high in plane spatial resolution with a subsequent thickness of the slices, which makes the use of the obtained image series difficult for 3D modeling. Besides, the cutting of the sample achieved to build the slices can deform the geometries, as shown in the works of Verbeek et al. [1] and of Dauguet et al. [2,3]. These deformations are incompatible with modeling since the model has to be as close as possible to the realistic geometries. Therefore, using a technique, which avoids cutting the sample for its structure observation, is mandatory.

Modeling the behavior of tissues does not only require information about the global structure of organs, but is also demanding for data about its microscopic constitution. In particular, it is usually accepted that collagen is the constituent which influences at most the mechanical behavior of living tissues as noted by Holzapfel and Ogden [4]. For modeling purposes, investigating the structure of the collagen network within tissues is therefore essential. In a recent work by our research group [5], the collagen network structure of cerebral bridging veins was investigated using histological slices. This work showed that the geometry of the vein was complex and not straight, which led to the impossibility of determining fiber orientations inside the vein wall on the prepared bi-dimensional slices. A 3D observation technique allowing the visualization of collagen fibers could give an answer to these issues encountered using histological slices.

Experimental techniques providing volume 3D images of the collagen structure of tissues do already exist in the literature. For example, we note the multiphoton fluorescence microscopy techniques [6–8], which have the advantage to avoid any preparation of the sample for the observation of collagen due to its autofluorescence. Another technique allowing such observations is second harmonic imaging microscopy [9–11]. Both of these techniques allow imaging the collagen network at the fiber scale (around one micron in resolution), but are restricted to small three-dimensional fields of view (at the most $500 \times 500 \times 200\ \mu m^3$), which do not allow for a global view of the organ geometry.

In the current work, we propose to use X-ray micro-CT (X-ray microtomography) for the observations of soft tissues. Such 3D observations have already been proposed in the literature by Metscher et al. [12–14], Johnson et al. [15], Wirkner and Prendini [16] but these studies focused on larger scales and on different applications. Pauwels et al. [17], Aslanidi et al. [18–20], Jeffery et al. [21] and Mizutani et al. [22] used high-Z element staining to investigate the structure of soft tissues at larger scales compared to those addressed by the present observations. Our work aims at the investigation of the collagen structure at the collagen fiber scale. Besides, it considers a piece of porcine vascular wall whereas most previous works focused rather on bigger organs or organisms.

Our technique, based on micro-CT, provides an isotropic 3D volume observation of the collagen structure in biological tissues. This technique focuses on a scale which is larger than those addressed by multiphoton fluorescence imaging and second harmonic imaging microscopy, but smaller than those previously studied using micro-CT. It does allow for fields of view of around $1500 \times 1500 \times 1500\ \mu m^3$, which enable a global overview of the tissue geometry. Therefore, our new observations technique fills a gap in the range of various techniques allowing volume 3D observations of soft tissues at multiple scales. Besides, thanks to the cone-beam geometry, the micro-CT imaging device provides images with isotropic voxels. This allows cutting the observed volume at a post-processing step without any deformation or interpolation computation. This point constitutes a real advantage in comparison to other imaging techniques. By keeping an intact sample, it avoids any deformation, which could be induced by a slicing procedure. The minimum voxel size of around one micron allows for the observation of collagen fibers.

Imaging the structure of tissues requires some contrast within the tissue. In the present work, we first checked if there was any native X-rays contrast between collagen and the other surrounding constituents of the vascular wall. We then used and compared three different stains through a preliminary observation using a preclinical micro-CT system. Even if the minimum voxel size of 25 μm reached by this system is unsuited to the observation of collagen fibers, it allows for a fast selection of relevant staining procedures. The most relevant staining procedure was then used to provide a detailed observation of the structure of the collagen network within a porcine vein wall sample.

## 2. Rationale

X-ray images contrast is based on a difference of attenuation within the several constituents of the tissue of interest. The attenuation law of an electromagnetic wave is exponential. Its expression is given, locally (for a limited area corresponding to a pixel of the detector for example), by:

$$I = I_0 \ \mathrm{e}^{-\mu x}$$

where $I$ is the intensity of the transmitted wave, $I_0$ is the intensity of the incident wave, $\mu$ is the attenuation coefficient of the constituent of the tissue, and $x$ is the abscissa of a point situated within the thickness of the material.

The contrast is generated by the differences of the attenuation coefficient $\mu$ from one point to another. This coefficient has been showed to depend principally on three parameters: the mean value of the atomic numbers of the target atoms, the energy of the incident photons (linked to their wavelength), and the density of the constituents of the tissue (also linked to their atomic numbers).

In case of soft tissues, the atoms composing the material have atomic numbers ($Z$), which are close from one to each other (the elements characteristics are given by Hubell and Seltzer [23]). Indeed soft tissues are mainly composed of hydrogen ($Z = 1$), carbon ($Z = 6$), oxygen ($Z = 8$) and nitrogen ($Z = 7$). Therefore, it is unlikely that a native difference of atomic number between the constituents can generate a sufficient contrast within the tissue.

In literature, some disparities exist between the density values commonly given for collagen and for the other constituents of vein walls. Densities ranging from 0.76 to 2.68 g/cm$^3$ (average of 1.6 g/cm$^3$) have been measured by Hashemi et al. [24] for collagen fibers. Similar values have been determined in the works of Hellmlich and Ulm [25], and Holmes and Kadler [26]. The density of the other constituents is closer to the one of water as noted by Anber et al. [27] and by Lillie and Gosline [28]. This difference of density from one constituent to another may generate a sufficient contrast between collagen fibers and the surrounding media when observed using X-rays. If it is not the case, contrast stains could be added to the sample to generate a sufficient contrast.

To investigate this point, different staining procedures were used in the present study. First, an unstained specimen was considered. This sample is used as reference. Then we used three different stains, based on those proposed by Metscher et al. [12–14] for the observation of small animals. These three stains are phosphotungstic acid (PTA), phosphomolybdic acid (PMA) and iodine potassium iodide (Lugol). We note that PTA and/or PMA intervene in the preparation of the Masson's trichrome solution classically used for the staining of collagen in histological slices. This denotes that these substances bind to the collagenous component of the soft tissue. This affirmation has also been proven in different works from the literature, for example in the works of Nemetschel et al. [29], Puchtler and Isler [30] or Watson [31]. Interestingly, these substances could also slightly color the elastin component of the tissue, as noted by Greenlee et al. [32].

Based on these considerations, we propose in the following an analysis of different sample preparations for the observation of the collagenous structure of the vein walls using micro-CT.

## 3. Methods

### 3.1. Micro-CT imaging systems

For the preliminary observation aiming at a selection of the relevant staining procedures, a pre-clinical X-ray micro-CT system (eXplore CT 120, GE Healthcare, Waukesha, USA) was used. This system can reach a minimum voxel size of $25 \times 25 \times 25$ μm$^3$.

For the detailed observation of a stained vein wall sample, a commercial system (Phoenix Nanotom s, GE Measurement and Control, Wunstorf, Germany) was used. This system can reach a minimum voxel size of $0.3 \times 0.3 \times 0.3$ μm$^3$, but its physical resolution is about 1 μm. We will present, in the second part of this paper, the results of an observation dealing with the maximum capabilities of this micro-CT system.

The acquisition parameters for both of these observations are summarized in Table 1.

### 3.2. Contrast stains and sample preparation

The proposed observations focus on the structure of vein walls. For a reason of ease of obtaining and of manipulation, we considered porcine iliac veins of around 6 mm in diameter. These samples were taken directly at a slaughterhouse. They were put in warm uncontrolled

**Table 1**
Micro-CT systems and acquisition parameters.

| | Preliminary observation | Detailed observation |
|---|---|---|
| X-ray Micro-CT system | GE Healthcare eXplore CT 120 | GE Measurements and Control, Phoenix Nanotom |
| Considered field of view | $10 \times 10 \times 10$ mm$^3$ | $1.3 \times 1.3 \times 1$ mm$^3$ |
| Current | 32 mA | 260 μA |
| Voltage | 80 kV | 100 kV |
| Exposure time | 100 ms | 1000 ms |
| Averaging | 1 | 3 |
| Number of projections | 1200 | 1440 |
| Reconstructed voxel size | $25 \times 25 \times 25$ μm$^3$ | $1 \times 1 \times 1$ μm$^3$ |

**Table 2**
Samples preparation and staining procedures.

| Contrast stain | PTA (phosphotungstic acid) | PMA (phosphomolybdic acid) | Lugol (iodine potassium iodide) | No staining (reference sample) |
|---|---|---|---|---|
| Fixation solution<br>Storage until staining | Formalin<br>Progressive dehydration until 70% alcohol | Formalin<br>Progressive dehydration until 70% alcohol | Formalin<br>Water | Formalin<br>Progressive dehydration until 70% alcohol. Kept into alcohol until observation |
| Preparation of the stain solution | Mix 30% of 1% phosphotungstic acid with 70% absolute ethanol | Mix 30% of 1% phosphomolybdic acid with 70% absolute ethanol | 1% Iodine metal + 2% potassium iodide + 97 mL of water. Dilute to 10% before use | – |
| Staining procedure | 70% alcohol<br>▼<br>Staining during one night<br>▼<br>Wash in 70% alcohol<br>▼<br>Conservation and observation in 70% alcohol | 70% alcohol<br>▼<br>Staining during one night<br>▼<br>Wash in 70% alcohol<br>▼<br>Conservation and observation in 70% alcohol | Water<br>▼<br>Staining during one night<br>▼<br>Wash in water<br>▼<br>Progressive dehydration in ethanol<br>▼<br>Conservation and observation in 70% alcohol | – |

water during transportation (at an initial temperature of 37 °C, decreasing until ambient temperature during transportation) to keep the sample hydrated. The surrounding conjunctive tissue was dissected within one hour after extraction. The samples were then fixed in a 10% formalin solution for one night and the different staining procedures were applied.

These staining procedures as well as the preparation of the staining solutions are detailed in Table 2. We note that PTA and PMA stains require the sample's dehydration, which is not the case of the Lugol stain [12–14]. The staining times were shown not to be critical as far as these times are sufficient for the staining solution to penetrate in the whole tissue. Nevertheless it has already been shown that the Lugol stain diffuses in most specimens in a few hours [12,17] whereas PTA and PMA include larger molecules, which need more time to penetrate into the tissue [17,33–36]. Our considered vein samples were small and thin (thickness of less than 1 mm). Taking into account the observations made by Pauwels et al. [17], who showed that PTA penetrates over a distance of 2.08 mm within the specimen for a staining duration of 24 h, we consider that stain penetration over duration of one night was sufficient for our samples.

Two vein samples extracted from different pigs were considered for a preliminary observation, leading to a comparison of three staining solutions (each vein was cut into four parts stained separately). The two samples associated with PTA staining were then cut and considered for the detailed observation.

### 3.3. Samples mounting

All of the samples were observed in an aqueous media composed of 70% alcohol. For the preliminary observation, 5 mm long portions of stained vein walls were inserted into Microtainer tubes of 8 mm in diameter (Becton, Dickinson and Company, USA) and then placed into the pre-clinical micro-CT system.

For the detailed observation, the need to reach a voxel size of around one cubic micron imposed reducing the sample size (see Fig. 1a). To achieve this, pieces of vein walls were cut lengthwise using a thin sharp blade. These specimens, composed of a 5-mm-long strip of vein wall, were inserted into a laboratory-made tube of 2 mm in diameter stuck on a steel rod using epoxy resin. This preparation is represented in Fig. 1b and is close to the one proposed by Mizutani et al. [22].

## 4. Results and discussion

First, a preliminary observation with a voxel size of $25 \times 25 \times 25\ \mu m^3$ using a pre-clinical micro-CT system was conducted. This observation provides a global view of the considered vein preparations. The results are shown in Fig. 2.

On the images given in Fig. 2a, we notice that the unstained reference sample does not show a strong contrast. The native difference of densities between the constituents of the tissue as well as with reference to the surrounding liquid are not strong enough to provide any useful contrast. Therefore some staining of the tissue is required. Fig. 2b shows a sample stained with Lugol's solution. On these images, we can distinguish two layers in the vein wall. These layers will be noticed again on the following images. PTA and PMA stained samples are shown respectively in Fig. 2c and d. The appearances of the images coming from these two stained samples are similar. Again, we notice two layers in the vein wall. These two layers deal with portions of the vessel wall, which have different collagen contents. They correspond with the media and adventitia composing most vessel walls. The intima layer is not visible since it is too thin. A thin layer of conjunctive tissue surrounding the vein can also be observed.

The contrasts obtained within the vein wall and with reference to each staining procedure are analyzed

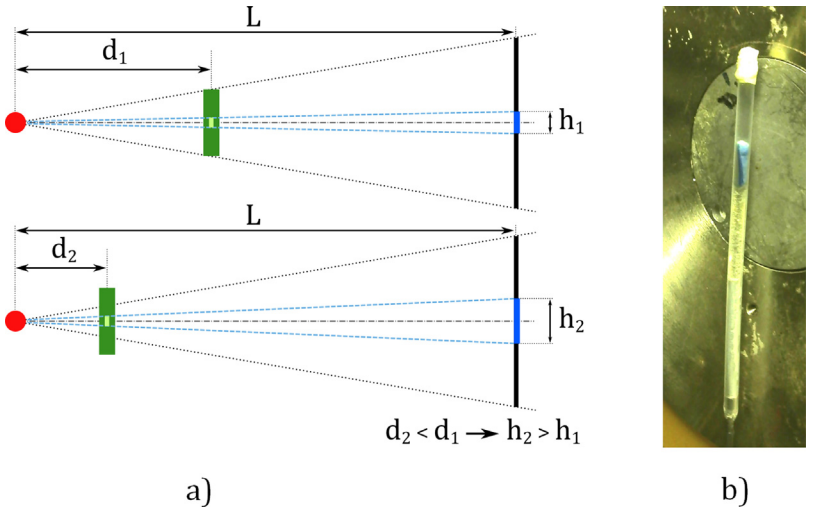


**Fig. 1.** (Color online) (a) Influence of the distance between the source and sample on the physical voxel size. Reducing the voxel size imposes to move the sample closer to the source: $d_2 < d_1$ leads to $h_2 > h_1$. Since the sample must rotate during acquisition, its size (or diameter) is limited. (b) Mounting arrangement of the tubes including the samples within the micro-CT device, and correspondence with (a). Detail of the tube of 2 mm in diameter for the detailed observation. The sample is positioned by gravity at the bottom of the tube.

quantitatively in Fig. 3 and Table 3. These profiles are plotted along an abscissa corresponding to a radius of the vein considered in circumferential cut after application of a Gaussian filter (smoothing radius of 3, filter implemented in Microview software, GE Healthcare). We notice on this figure that the differences of grey levels are much higher in the case of PMA and PTA staining. Since PTA and PMA staining seem to lead to similar contrasts, we will only focus on the PTA stained sample in the following.

Fig. 4 shows a detailed observation of a sample stained with PTA. The voxel size for the observed volume is of $1 \times 1 \times 1\ \mu m^3$. In this figure, a three-dimensional visualization of the vein wall sample is given. Three orthogonal slices associated in different planes are also proposed. The medial and adventitial layers, previously detected in Fig. 2b, c, d, are clearly visible. A thin piece of conjunctive tissue, which has not been removed during the vein dissection, surrounds the vein wall.

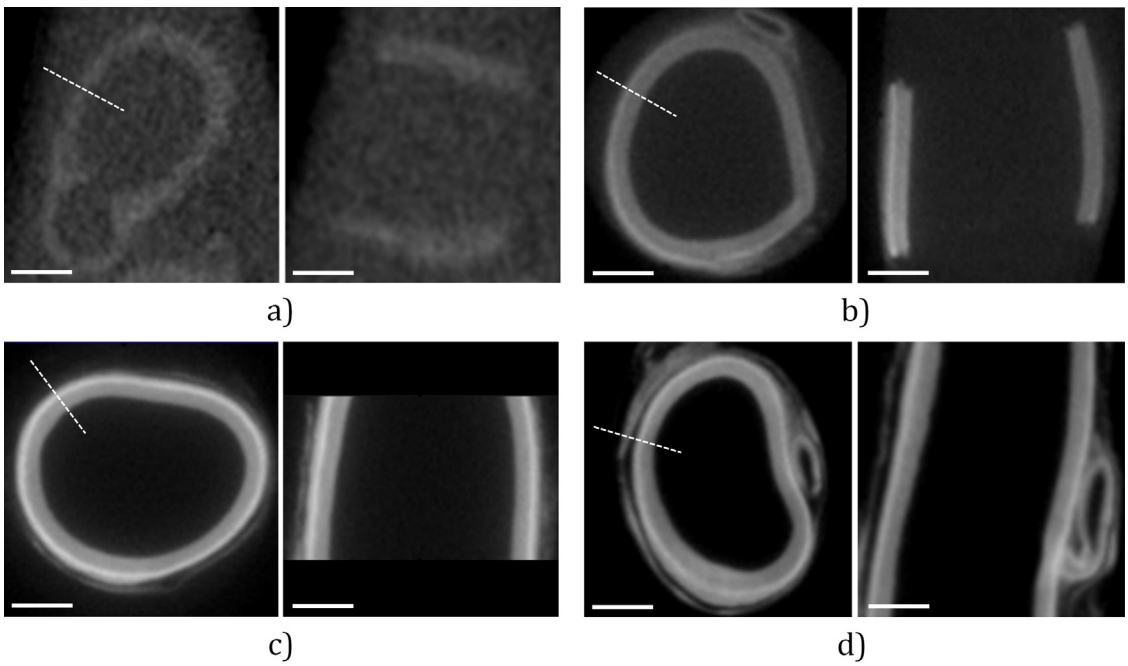


**Fig. 2.** Comparison of the different proposed staining procedures. The voxel size for these observations is 25 μm (cubic voxels). For each sample, a circumferential (left image) and a longitudinal cut (right image) of the vessel are given. (a) Reference sample (unstained). (b) Lugol staining. (c) PMA staining. (d) PTA staining. The scale bars are 2 mm. The dotted lines deal with the grey level profiles showed in Fig. 3.

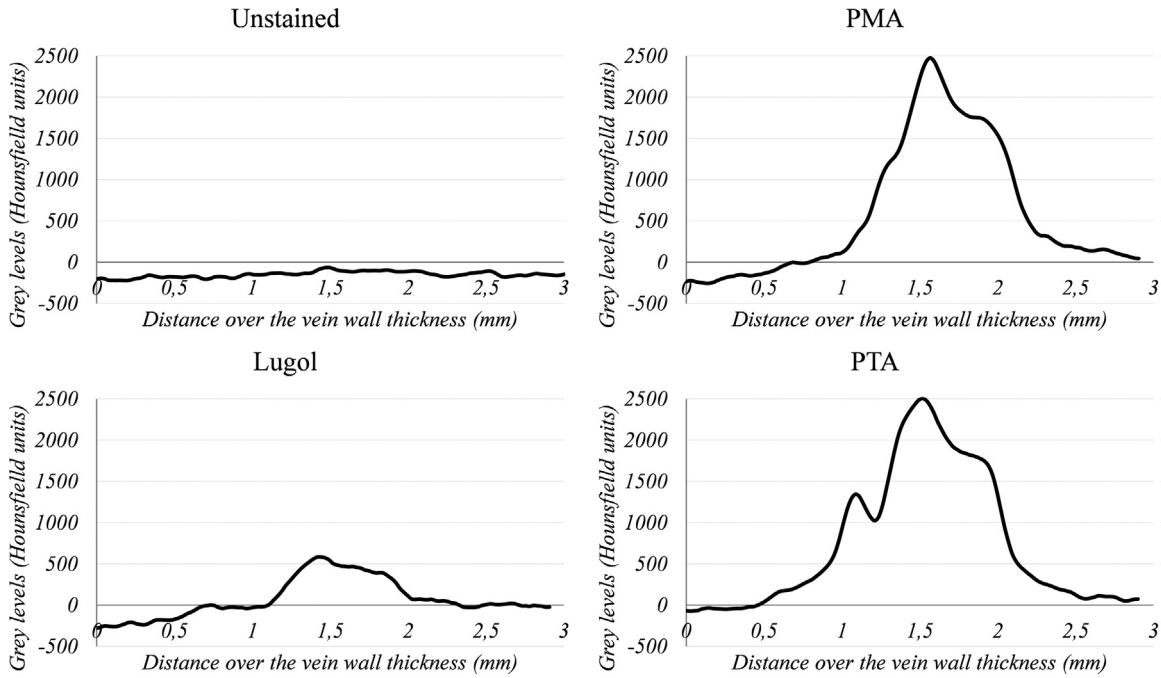


**Fig. 3.** Grey level profiles (in Hounsfield units) along the thickness of the vein wall showing the contrast obtained with the different stains. The profiles are plotted after applying a Gaussian filter on the considered images to avoid the contribution of noise. The Hounsfield scale was obtained by a specific calibration procedure performed on the micro-CT. The lines defining the profiles associated with these curves are showed in Fig. 2 (0 mm deals with a point outside the vessel and 3 mm deals with a point inside the lumen of the vein).

Small black dots are also visible in the adventitial layer of the vein wall, which correspond to the vasa vasorum. This vasa vasorum has already been observed at a larger scale by the research team of Ritman et al. [37–39]. It constitutes a network of small vessels that supplies the walls of larger blood vessels. The geometry of the vasa vasorum network was extracted and is shown in Fig. 5.

The voxel size of one cubic micron allows for the observation of small collagen fibers, which are mainly visible in the adventitia in the *X*–*Z* view. We show in Fig. 6a a tangential slice that uses a Minimum Intensity Projection (MinIP) over 40 images (corresponding to images over a thickness of 40 μm), which shows the vasa vasorum. MinIP projection consists of a projection of a volume of interest to generate a bidimensional image, where the projections of the voxels keep only the lowest attenuation value on every view. In Fig. 6c, which is another tangential slice, we notice that the medial layer includes collagen fibers, which are oriented circumferentially whereas these fibers are longitudinally arranged in the adventitia. Nevertheless, these orientations can correspond to helically arranged collagen fibers with respectively small and high (close to 90°) helix angles. The orientations of collagen fibers resulting from this observation are shown in Fig. 7. The obtained fiber orientations are in accordance with observations, performed by other research teams on different vessels, for example by Watts et al. [40] on rats aortas and vena cava.

By comparing the average grey levels in the different layers of the vein wall (see Figs. 2, 4 and 6), it is possible to assess qualitatively the relative proportion of collagen in each layer. By this way, it is noticeable that the adventitia has a larger collagen density compared to the media. This observation is in accordance with the work of Holzapfel [41] focused on arterial walls.

Our study also allowed assuming the stability of the PTA staining. The same sample was observed several times within 10 months leading no significant loss of contrast on the obtained images. Therefore, we can affirm that the PTA staining remains stable. This observation is in accordance with the results of Pauwels et al. [17], which showed no contrast variation after 4 days of conservation of the sample in water.

**Table 3**
Attenuation coefficient difference between two structures in Hounsfield units.

| Values in HU | Unstained | Lugol | PMA | PTA |
|---|---|---|---|---|
| Media vs. background | 61 | 411 | 1753 | 1840 |
| Adventice vs. background | 61 | 502 | 2299 | 2452 |
| Adventice vs. media | 0 | 91 | 546 | 613 |

The mean standard deviation of measures taken in 11 regions of interest is of 163HU, which allows the exclusion of Lugol staining as a relevant stain, regarding a signal to noise ratio as well as an adventice/media contrast criterion.

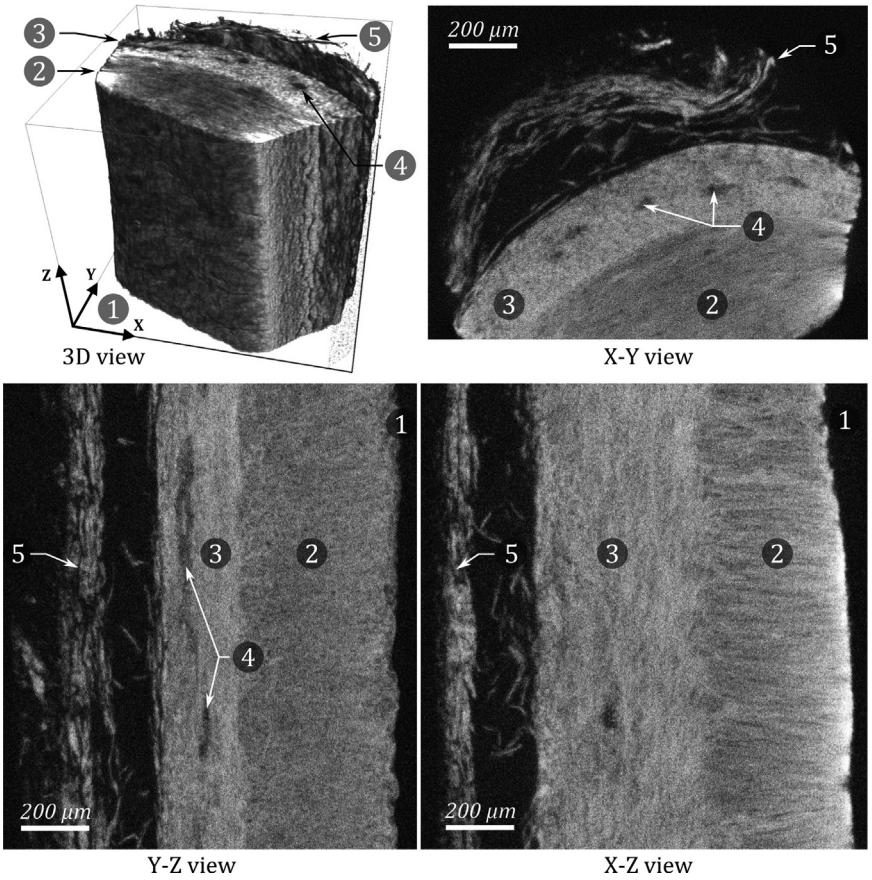


**Fig. 4.** Different views of a small sample of PTA stained vein wall. This sample is included in a tube of 2 mm in diameter. We notice clearly fiber orientations in the different views. 1. Lumen of the vein. 2. Media. 3. Adventitia. 4. Vasa vasorum. 5. Surrounding conjunctive tissue. The observed volume has approximately $1300 \times 1300 \times 1000$ µm$^3$.

We note that the Masson's trichrome staining procedure involves PMA/PTA. This allows observing a Masson's trichrome stained sample embedded in paraffin using micro-CT. However, in our experience, we noticed that the surrounding paraffin degrades the global contrast by adding on the images a uniform non-negligible grey-level all around the sample (data not shown).

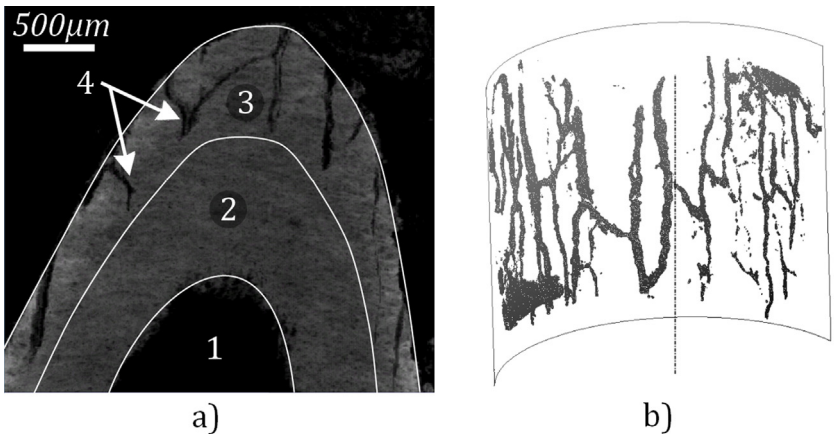


**Fig. 5.** (a) Highlighting of the vasa vasorum in the vein wall. This cut is inclined with reference to the vein axis. The two layers composing the vein wall could be distinguished and the vasa vasorum is only seen in the adventitial layer. The numbers deal with those defined in Fig. 4. The scale bar is 500 µm. (b) Three-dimensional geometry of the vasa vasorum network extracted from the images of the PTA stained sample.

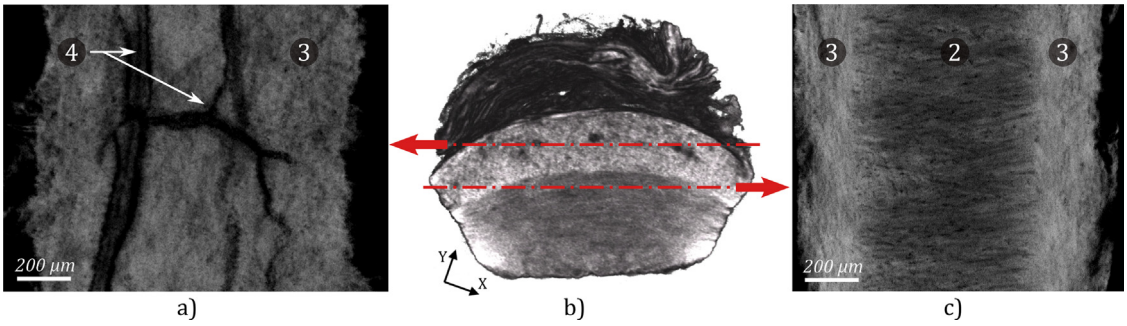


**Fig. 6.** (Color online.) (a) MinIP projection of 40 tangential slices at different locations in the vein wall. Tangential cut of the adventitial layer showing the vasa vasorum structure. (b) Localization of the two slices of Figs. (a) and (c). Tangential cut of the medial layer of the vein wall. Collagen fiber circumferential orientations are visible. This slice shows also the structure of the adventitial layer corresponding to rather longitudinal collagen fibers. The numbers deal with those defined in Fig. 4.

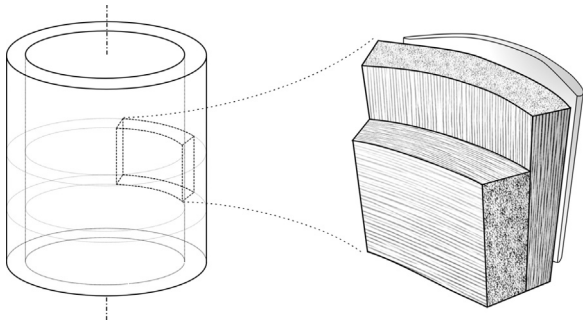

**Fig. 7.** Schematic representation of the observed portion of iliac vein wall. The collagen fibers embedded within the specimen stained with PTA are represented with circumferential orientations in the medial layer and longitudinal orientations in the adventitia. A piece of conjunctive tissue surrounds the vein wall.

In our work, we used the staining solutions previously used by Metscher et al. [12–14]. Our results showed as well that PTA and PMA staining were satisfactory in the case of vein walls, and for staining and observing the microscopic collagen network structure. Iodine potassium iodide (Lugol) staining led to good results in the works of Metscher et al. [12,13], even if the structures of the tissue were differently contrasted in comparison with PTA stained samples [12]. In our case, we showed that Lugol did not lead to a satisfactory contrast between the layers of the vessel wall. Therefore we can suppose that this solution does not stain collagen at most, but also stains other constituents of the tissue, like for example muscle fibers as showed by Jeffery et al. [21].

Pauwels et al. [17] obtained satisfactory contrast within the tissue using PTA and PMA staining. This observation is in accordance with our work, even if our study focuses on smaller scales. We note that Pauwels et al. [17] observed some slight precipitation at the surface of their samples. They were attributed to the high concentration of the staining solutions, which were used. In our work we used lower concentrations and did not observe these precipitations.

## 5. Conclusion

In the present work, a three-dimensional volume observation of the collagenous structure of a vascular soft tissue was achieved using micro-CT. We used fresh porcine iliac veins, which were stained with PTA, PMA and Lugol, which act as contrast agents, revealing the collagenous structures. The comparison of these three staining solutions showed that PTA and PMA lead to the best contrast within the tissue. Our work allowed the observation of the media and adventitia in the vein wall. The intima layer, which remains too thin, could not be observed. In the two observed layers of porcine iliac veins, collagen fibers were visible. They were shown to be circumferentially arranged in the media and to be longitudinally orientated in the adventitia. The vasa vasorum was also visible in the acquired images and the architecture of its network was extracted from these images. Our observation also allowed for a qualitative evaluation of the volume fraction of collagen from one part of the tissue to another.

Finally, the proposed observation technique and staining procedures allow imaging the collagen structure of the tissue with a voxel size of around one micron. One of the advantages of this technique relies in the fact that it does still allow for fields of view of several cubic millimeters and for isotropic voxels, which make post-processing easier. By this way, it is situated at a larger scale than multiphoton microscopy, but does still allow detailed three-dimensional observations of the structure of the tissue.

## Disclosure of interest

The authors declare that they have no conflicts of interest concerning this article.

## Acknowledgements

The authors would like to thank J.-M. Hiver and O. Ferry from the *École des mines de Nancy* as well as G. Fargier from the *École centrale de Lyon* (Equipex IVTV) for their help to the observation using the microtomographs. They would also thank A. Sayeh for her help using the preclinical micro-CT system.

## Appendix A. Supplementary data

Supplementary data associated with this article can be found, in the online version, at http://dx.doi.org/10.1016/j.crvi.2015.04.009.

## References


[1] F.J. Verbeek, D.P. Huijsmans, R.J.M. Baeten, N.J.C. Schoutsen, W.H. Lamers, Design and implementation of a database and program for 3D reconstruction from serial sections: a data-driven approach, Microsc. Res. Techniq. 30 (1995) 496–512.

[2] J. Dauguet, T. Delzescaux, F. Cond, J.F. Mangin, N. Ayache, P. Hantraye, V. Frouin, Three-dimensional reconstruction of stained histological slices and 3D non-linear registration with in-vivo MRI for whole baboon brain, J. Neurosci. Meth. 164 (2007) 191–204.

[3] J. Dauguet, L'imagerie post-mortem tridimensionnelle cérébrale : constitution et apport pour l'analyse conjointe de données histologiques anatomo-fonctionnelles et la mise en correspondance avec l'imagerie in vivo, (PhD. Dissertation), École centrale de Paris, France, 2005.

[4] G.A. Holzapfel, R.W. Ogden, Biomechanics of soft tissue in cardiovascular systems, Springer, Wien, Austria, 2003.

[5] M. Nierenberger, R. Wolfram, S. Decock, N. Boehm, Y. Rémond, J.L. Kahn, S. Ahzi, Investigation of the human bridging veins structure using optical microscopy, Surg. Radiol. Anat. 35 (2012) 331–337.

[6] R. Cicchi, D. Kapsokalyvas, V. De Giorgi, V. Maio, A. Van Wiechen, D. Massi, T. Lotti, F.S. Pavone, Scoring of collagen organization in healthy and diseased human dermis by multiphoton microscopy, J. Biophotonics 3 (2010) 34–43.

[7] K. König, K. Schenke-Layland, I. Riemann, U.A. Stock, Multiphoton autofluorescence imaging of intratissue elastic fibers, Biomaterials 26 (2005) 495–500.

[8] C.B. Raub, V. Suresh, T. Krasieva, J. Lyubovitsky, J.D. Mih, A.J. Putnam, B.J. Tromberg, S.C. George, Noninvasive assessment of collagen gel microstructure and mechanics using multiphoton microscopy, Biophys. J. 92 (2007) 2212–2222.

[9] E. Brown, T. McKee, E. diTomaso, A. Pluen, B. Seed, Y. Boucher, R.K. Jain, Dynamic imaging of collagen and its modulation in tumors in vivo using second-harmonic generation, Nat. Med. 9 (2003) 796–800.

[10] G. Cox, E. Kable, A. Jones, I. Fraser, F. Manconi, M.D. Gorrell, 3-Dimensional imaging of collagen using second harmonic generation, J. Struct. Biol 141 (2003) 53–62.

[11] M. Han, G. Giese, J. Bille, Second harmonic generation imaging of collagen fibrils in cornea and sclera, Opt. Express 13 (2005) 5791–5797.

[12] B. Metscher, MicroCT for comparative morphology: simple staining methods allow high-contrast 3D imaging of diverse non-mineralized animal tissues, BMC Physiol. 9 (1) (2009) 11.

[13] B.D. Metscher, MicroCT for developmental biology: A versatile tool for high-contrast 3D imaging at histological resolutions, Dev. Dynam. 238 (2009) 632–640.

[14] B.D. Metscher, G.B. Müller, MicroCT for molecular imaging: Quantitative visualization of complete three-dimensional distributions of gene products in embryonic limbs, Dev. Dynam. 240 (2011) 2301–2308.

[15] J.T. Johnson, M.S. Hansen, I. Wu, L.J. Healy, C.R. Johnson, G.M. Jones, M.R. Capecchi, C. Keller, Virtual histology of transgenic mouse embryos for high-throughput phenotyping, PLoS Genet. 2 (2006) e61.

[16] C.S. Wirkner, L. Prendini, Comparative morphology of the hemolymph vascular system in scorpions–A survey using corrosion casting, MicroCT, and 3D-reconstruction, J. Morphol 268 (2007) 401–413.

[17] E. Pauwels, D. Van Loo, P. Cornillie, L. Brabant, L. Van Hoorebeke, An exploratory study of contrast agents for soft tissue visualization by means of high resolution X-ray computed tomography imaging, J. Microsc. 250 (2013) 21–31.

[18] O.V. Aslanidi, T. Nikolaidou, J. Zhao, B.H. Smaill, S.H. Gilbert, A.V. Holden, T. Lowe, P.J. Withers, R.S. Stephenson, J.C. Jarvis, J.C. Hancox, M.R. Boyett, H. Zhang, Application of micro-computed tomography with iodine staining to cardiac imaging, segmentation, and computational model development, IEEE Trans. Med. Imaging 32 (2013) 8–17.

[19] M. Vorpahl, J.R. Foerst, M. Kelm, A.V. Kaplan, R. Virmani, T. Ball, The complementary role of microCT and histopathology in characterizing the natural history of stented arteries, Expert. Rev. Cardiovasc. Ther. 9 (2011) 939–948.

[20] O.V. Aslanidi, M.A. Colman, M. Varela, J. Zhao, B.H. Smaill, J.C. Hancox, M.R. Boyett, H. Zhang, Heterogeneous and anisotropic integrative model of pulmonary veins: computational study of arrhythmogenic substrate for atrial fibrillation, Interface Focus 3 (2013).

[21] N.S. Jeffery, R.S. Stephenson, J.A. Gallagher, J.C. Jarvis, P.G. Cox, Micro-computed tomography with iodine staining resolves the arrangement of muscle fibres, J. Biomech. 44 (2011) 189–192.

[22] R. Mizutani, Y. Suzuki, X-ray microtomography in biology, Micron 43 (2012) 104–115.

[23] J.H. Hubbell, S.M. Seltzer, NIST: X-Ray Mass Attenuation Coefficients. US Department of Commerce, 1995 Available at: http://www.nist.gov/pml/data/xraycoef/index.cfm/What. Accessed 2 May, 2014.

[24] J. Hashemi, N. Chandrashekar, J. Slauterbeck, The mechanical properties of the human patellar tendon are correlated to its mass density and are independent of sex, Clin. Biomech. 20 (2005) 645–652.

[25] C. Hellmich, F.J. Ulm, Are mineralized tissues open crystal foams reinforced by crosslinked collagen? Six some energy arguments, J. Biomech. 35 (2002) 1199–1212.

[26] D.F. Holmes, K.E. Kadler, The 10 + 4 microfibril structure of thin cartilage fibrils, Proc. Natl. Acad. Sci. USA 103 (2006) 17249–17254.

[27] V. Anber, B.A. Griffin, M. McConnell, C.J. Packard, J. Shepherd, Influence of plasma lipid and LDL-subfraction profile on the interaction between low density lipoprotein with human arterial wall proteoglycans, Atherosclerosis 124 (1996) 261–271.

[28] M.A. Lillie, J.M. Gosline, Unusual swelling of elastin, Biopolymers 64 (2002) 115–126.

[29] T. Nemetschek, H. Riedl, R. Jonak, Topochemistry of the binding of phosphotungstic acid to collagen, J. Mol. Biol. 133 (1979) 67–83.

[30] H. Puchtler, H. Isler, The effect of phosphomolybdic acid on the stainability of connective tissues by various dyes, J. Histochem. Cytochem. 6 (1958) 265–270.

[31] M.L. Watson, Staining of tissue sections for electron microscopy with heavy metals, J. Biophys. Biochem. Cytol. 4 (1958) 475–478.

[32] T.K. Greenlee, R. Ross, J.L. Hartman, The fine structure of elastic fibers, J. Cell Biol. 30 (1966) 59–71.

[33] R.E. Golding, A.S. Jones, Micro-CT as a novel technique for 3D reconstruction of molluscan anatomy, Molluscan. Res. 27 (2007) 123–128.

[34] R.E. Golding, W.F. Ponder, M. Byrne, Three-dimensional reconstruction of the odontophoral cartilages of Caenogastropoda (Mollusca: Gastropoda) using micro-CT: Morphology and phylogenetic significance, J. Morphol. 270 (2009) 558–587.

[35] M.A. Hayat, Principles and techniques of electron microscopy: biological applications, Cambridge University Press, Cambridge, UK, 2000.

[36] J.A. Kiernan, Histological and histochemical methods: theory and practice, Shock 12 (1999) 479.

[37] H.M. Kwon, G. Sangiorgi, E.L. Ritman, C. McKenna, D.R. Holmes, R.S. Schwartz, A. Lerman, Enhanced coronary vasa vasorum neovascularization in experimental hypercholesterolemia, J. Clin. Invest. 101 (1998) 1551–1556.

[38] E.L. Ritman, A. Lerman, The dynamic vasa vasorum, Cardiovasc. Res. 75 (2007) 649–658.

[39] M. Gössl, M. Rosol, N.M. Malyar, L.A. Fitzpatrick, P.E. Beighley, M. Zamir, E.L. Ritman, Functional anatomy and hemodynamic characteristics of vasa vasorum in the walls of porcine coronary arteries, Anat. Rec. 272A (2003) 526–537.

[40] S.W. Watts, C. Rondelli, K. Thakali, X. Li, B. Uhal, M.H. Pervaiz, R.E. Watson, G.D. Fink, Morphological and biochemical characterization of remodeling in aorta and vena cava of DOCA-salt hypertensive rats, Am. J. Physiol. Heart Circ. Physiol. 292 (2007) H2438–H2448.

[41] G.A. Holzapfel, G. Sommer, C.T. Gasser, P. Regitnig, Determination of layer-specific mechanical properties of human coronary arteries with nonatherosclerotic intimal thickening and related constitutive modeling, Am. J. Physiol. Heart C 289 (2005) 2048–2058.